NJC

Accepted Manuscript

This is an *Accepted Manuscript*, which has been through the Royal Society of Chemistry peer review process and has been accepted for publication.

Accepted Manuscripts are published online shortly after acceptance, before technical editing, formatting and proof reading. Using this free service, authors can make their results available to the community, in citable form, before we publish the edited article. We will replace this *Accepted Manuscript* with the edited and formatted *Advance Article* as soon as it is available.

You can find more information about *Accepted Manuscripts* in the Information for Authors.

Please note that technical editing may introduce minor changes to the text and/or graphics, which may alter content. The journal's standard Terms & Conditions and the Ethical guidelines still apply. In no event shall the Royal Society of Chemistry be held responsible for any errors or omissions in this *Accepted Manuscript* or any consequences arising from the use of any information it contains.

ROYAL SOCIETY OF CHEMISTRY

www.rsc.org/njc

Cite this: DOI: 10.1039/c0xx00000x

www.rsc.org/xxxxxx

ARTICLE TYPE

A highly stable *double-coordinated* 2-hydroxy-tri(*tert*-butyl)-substituted zinc phthalocyanine dimer: synthesis, spectral study, thermal stability and electrochemical properties

Alexander Yu. Tolbin,[*a] Victor E. Pushkarev,[a] Irina O. Balashova,[a] Alexander V. Dzuban,[b] Pavel A. Tarakanov,[a] Stanislav A. Trashin,[a] Larisa G. Tomilova,[a,b] and Nikolay S. Zefirov[a,b]

Received (in XXX, XXX) Xth XXXXXXXXX 20XX, Accepted Xth XXXXXXXXX 20XX
DOI: 10.1039/b000000x

A highly stable J-type dimer based on 2-hydroxy-tri(*tert*-butyl)-substituted zinc phthalocyanine with specific supramolecular architecture was investigated by UV-visible, fluorescence spectroscopy and cyclic voltammetry to show strong π–π interactions and coordination between hydroxy-groups and Zn^{2+} central metal ions. The possibility of controlling the fluorescent properties of the obtained complex by using of different solvents is demonstrated, which along with high thermal stability according to thermoanalytical study may increase practical applicability of supramolecular dimeric phthalocyanine compounds.

The significant advances in supramolecular chemistry of macroheterocyclic compounds have stimulated a numerous studies on aggregation processes to explain some features that are unusual for single molecules [1]. For a long time, phthalocyanines have the attracted attention of researchers owing to their unique optical and electrical properties, resulting in investigations of these compounds in the area of optical physics, in particular, regarding non-linear optical properties and the ability to transfer energy upon excitation. They possess promising technological capability in the fields related to preparation of organic semiconductors and chemical sensors, as well as materials for laser technologies, photovoltaic devices and medicine [2]. These macrocyclic dyes are excellent building blocks for supramolecular self-assembly, demonstrating significant changes in the spectral properties of the resulting aggregates [3-6]. In this connection a great attention is paid to investigation of the head-to-tail dimers, which usually represent the J-type aggregates, since they show strong fluorescence properties compared to the face-to-face dimers of H-type [7]. However, in most cases, such associates are not sufficiently stable. They can be formed exceptionally in non-polar solvents [7-9] as well as in the presence of heavy metal ions [10-12] or upon irradiation [13]. In this connection, the few published works are mainly focused on studying the dimer–monomer equilibrium by the UV–Vis and fluorescence spectroscopy during dissociation of the dimers upon addition of coordinating solvents or reagents [3, 8, 10, 14]. Recently, we reported on the first synthesis of highly stable J-type dimer based on 2-hydroxy-tri(*tert*-butyl)-substituted zinc phthalocyanine [15]. In the present work a comprehensive study of the physicochemical properties of this dimeric complex are discussed in order to determine the reasons for its considerable stability with potentially broad applications in material science.

Experimental

General methods

All solvents were reagent-grade quality and were obtained from Aldrich. Phthalocyanine ligand **1** was synthesized according to our previously published procedures [16]. UV–Vis spectra were recorded on a Hitachi U-2900 spectrophotometer in a range of 190-1100 nm in toluene, THF, pyridine and conc. sulfuric acid. FT–IR spectra were recorded in KBr pellets on a Nicolet Nexus IR-Furje spectrometer. ^{1}H NMR (400.13 MHz) spectra were recorded using a Bruker 400 NMR spectrometer. MALDI–TOF/TOF measurements were performed with a Bruker ULTRAFLEX II TOF/TOF spectrometer using 2,5-dihydroxybenzoic acid (DHB, Aldrich). Fluorescence emission and excitation spectra were obtained on a Varian Cary Eclipse Fluorescence Spectrophotometer. The fluorescence quantum yields (Φ_F) were estimated using PcZn in 1-propanol as a reference (λ_{ex} = 600 nm, Φ_F=0.45) [17]. The composition of complexes **2** and **3** was checked with a Perkin–Elmer 240 elemental analyser. Thermogravimetric (TG) and differential calorimetric analyses (DSC) were carried out on Netzsch STA 409 PC Luxx® thermal analyzer and Netzsch DSC 204 F1 Phoenix® differential scanning calorimeter correspondingly. TG measurements were performed in alumina crucible (lid with hole) under an argon flow with a heating rate of 10°C/min up to 800°C. DSC measurements were performed in aluminum crucible sealed with lids with holes under an air flow with a heating rate of 10°C/min up to 600°C. Electrochemical measurements were carried out with μAutolab II potentiostat controlled by Nova 1.8 software package (Metrohm Autolab B.V., The Netherlands). Cyclic voltammetry (CV) was performed in a conventional three-

electrode cell with a Pt-disk (2.0 mm in diameter) working and Pt-foil counter electrodes. *o*-Dichlorobenzene (DCB, for synthesis, Merck) purified by passing through a short Al_2O_3 column was used as a solvent, and 0.15 mol/L of Bu_4NBF_4 (Sigma-Aldrich, dried under vacuum at 80°C) as a supporting electrolyte. The saturated calomel reference electrode (SCE) was connected to the solution through a salt bridge. Liquid junction potentials were corrected to a ferrocenium$^+$/ferrocene couple (Fc^+/Fc, +0.49 V vs. SCE). The solution was purged with nitrogen for at least 20 min before measurements were taken. All measurements were performed at an ambient temperature (22 ± 1°C).

Syntheses

2-Hydroxy-9(10),16(17),23(24)-tri-*tert*-butyl-29H,31H-phthalocyanine [zinc](2). To a solution of **1** (0.430 g, 0.62 mmol) in DCB (8 mL), DBU (0.1 mL) and $Zn(OAc)_2{\times}2H_2O$ (0.150 g, 0.68 mmol) were added followed by keeping of the temperature under reflux for 40 min. Then, the reaction mixture was evaporated and the crude product was treated with aqueous methanol (2×50 mL) to remove residual amounts of DCB. Yield: 0.460 g, 98%. Anal. Calc. for $C_{44}H_{40}N_8OZn$: C, 69.33; N, 14.70; H, 5.29%. Found: C, 69.14; N, 14.64 and H, 5.32%. FT–IR (cm^{-1}): 3760–3250 (OH), 2954 (CH–Ar). MS (MALDI–TOF/TOF): *m/z* (I, %) 760.2622 (100%), exact ms. 760.2617. ^{1}H NMR (THF-d_8) δ/ppm: 1.73 (s, 27H, *tert*-Bu), 7.60 (d, 1H, β^o-H, *J*=8.4Hz), 8.28 (d, 3H, β-H, *J*=8.00Hz), 8.77 (s, 1H, α'^{o}-H), 9.29 (m, 1H, α^o-H), 9.29–9.44 (m, 3H, α-H), 9.46-9.59 (br. s, 3H, α'-H). UV–Vis λ_{max} (nm) (log ε) in toluene: 286 (3.53), 348 (3.93), 612 (3.65), 679 (4.34); in THF: 287 (3.82), 345 (4.19), 608 (3.85), 675 (4.52); in pyridine: 352 (4.19), 616 (3.85), 682 (4.48); in H_2SO_4: 292, 310, 445, 816. Fluorescence data: excitation λ_{max} (THF) 600 nm, emission λ_{max} = 682 nm, Stokes shift 7 nm, Φ_F=0.33; excitation λ_{max} (pyridine) 600 nm, emission λ_{max} = 697 nm, Stokes shift 9 nm, Φ_F=0.19.

Bis(2-hydroxy-9(10),16(17),23(24)-tri-*tert*-butyl-29H,31H-phthalocyanine [zinc]) (3). To a solution of **1** (0.400 g, 0.53 mmol) in DCB (8 mL), CH_3OLi (0.100 g, 2.65 mmol) was added followed by keeping of the mixture under reflux for 20 min. After that $Zn(OAc)_2{\times}2H_2O$ (0.232 g, 1.06 mmol) was added, and the mixture was refluxed for 30 min. After the reaction was finished, the solvent was evaporated and the crude product was treated with aqueous methanol (2×50 mL) followed by chromatographic purification on Bio-Beads SX-1 (THF as eluent) to give target dimeric product **3** as dark-blue powder. Yield: 0.348 g, 80%. Anal. Calc. for $C_{88}H_{80}N_{16}O_2Zn_2$: C, 69.33; N, 14.70; H, 5.29%. Found: C, 69.21; N, 14.61 and H, 5.28%. FT–IR (cm^{-1}): 3780–3230 (OH), 2960 (CH–Ar). MS (MALDI–TOF/TOF): *m/z* (I, %) 1522.5236 (100%), exact ms. 1524.5233. ^{1}H NMR (THF-d_8) δ/ppm: 1.76-2.26 (br. m, 54H, *tert*-Bu), 6.90–10.22 (br. m, 24H, Ar). UV–Vis λ_{max} (nm) (log ε) in toluene: 286 (3.65), 348 (4.03), 624 (3.72), 675 (4.29), 700 (4.17); in THF: 287 (3.86), 345 (4.22), 622 (3.89), 673 (4.38), 694 (4.29); in pyridine: 295 (3.69), 352 (4.06), 622 (3.77), 682 (4.33), 705 (4.21); in H_2SO_4: 312, 452, 809, 890. Fluorescence data: excitation λ_{max} (THF) 600 nm, emission λ_{max} = 695 nm, Stokes shift 22 nm, Φ_F=0.10; excitation λ_{max} (pyridine) 600 nm, emission λ_{max} = 697 nm, Stokes shift 5 nm, Φ_F=0.12.

Theoretical calculations

Theoretical calculations with ground state (S_0) geometry optimization of the model structures based on dimeric complex **3** were performed with density functional theory (DFT) method. Perdew–Burke–Ernzerhof (PBE) [18] functional and PRIRODA package [19] supplied with three exponent TZ2P basis set including twice polarized Gauss-type functions were used. The size of the basis set used is – (11s6p2d):[6s3p2d] for C and N, (5s5p2d):[3s3p2d] for O, (5s1p):[3s1p] for H and (17s13p8d):[12s9p4d] for Zn atom correspondingly. For the S_1 state, optimization of the geometries based on RHF–CIS calculations (3-21+G* basis set) was performed with GAMESS (US) package starting from optimized geometries for the S_0 state.

Results and discussion

Formation, spectral and structural features

The successive reaction of 2-hydroxy-9(10),16(17),23(24)-tri-*tert*-butylphthalocyanine ligand (**1**) with lithium methoxide and zinc acetate in DCB led to the formation of highly stable dimeric zinc complex **3** (Scheme 1). In the MALDI TOF/TOF mass spectrum only one peak with *m/z* 1522.5236 was detected, which is characteristic for the molecular ion of the desired product ([M–2H]$^+$). In the ^{1}H NMR spectrum, the signals belonging to the aromatic protons are strongly broadened and are observed over a wide range (7–10 ppm), which characterizes the tendency of macrocycles to establish strong intramolecular interactions (Supporting information, Figs S1-S4). However, when employing 1,8-diazabicycloundec-7-ene (DBU) as a base, only monomer complex **2** was obtained.

Cite this: DOI: 10.1039/c0xx00000x

www.rsc.org/xxxxxx

ARTICLE TYPE

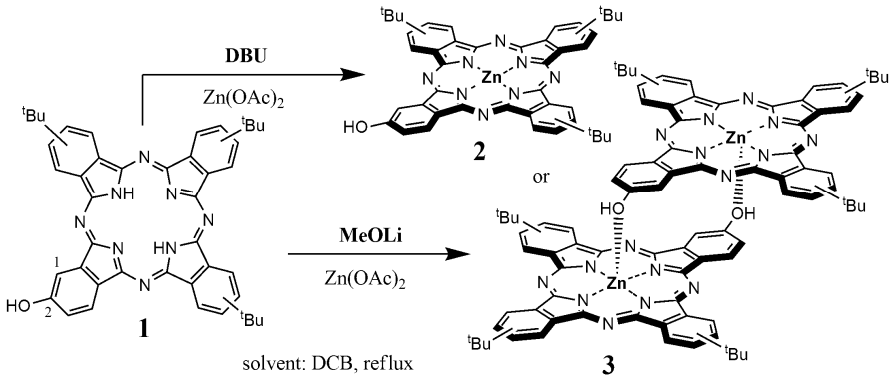

Scheme 1. The influence of the base nature for the selective formation of monomer **2** and dimer **3** complexes in DCB.

In the UV–Vis spectra of the dimeric complex **3**, which were obtained in non-polar and polar coordinating solvents, in addition to the traditional Q- and B-bands, a long-wavelength band near 700 nm was also observed (Fig. 1). For dimers, the appearance of this band is associated with the fact that the transitions to the upper and lower states of the electric dipole-dipole interaction level are allowed [20]. This band is referred to as a J-band, and is characteristic of dimers and aggregates in which the macrocycles are displaced relative to each other. For J-type dimers, the angle of slippage (θ) must be smaller than the critical value of 54.7° [21]. In turn, the monomeric complex shows the typical characteristics of the absorption spectrum for metal-containing phthalocyanines.

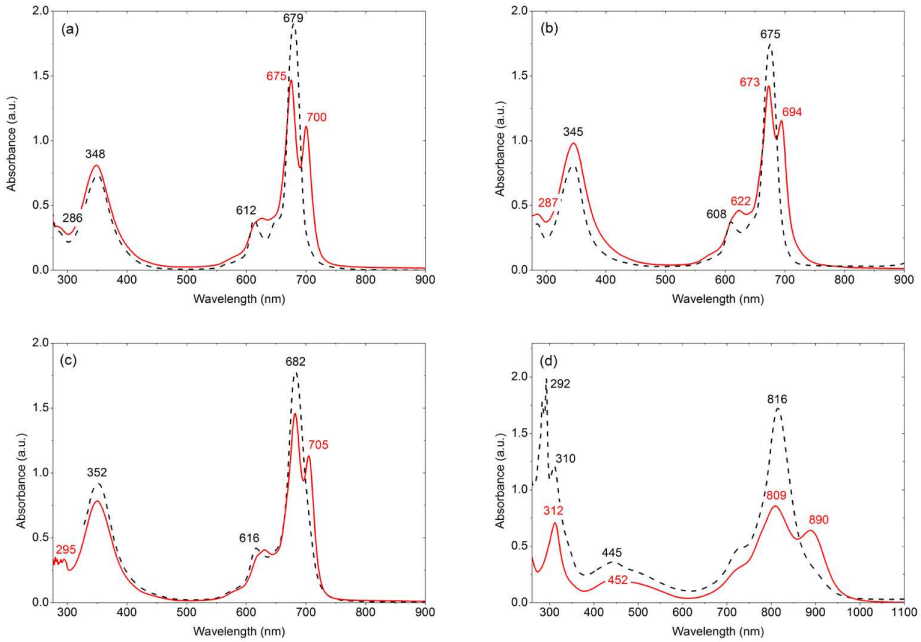

Fig. 1. UV–Vis spectra of complexes **2** (----) and **3** (——) in toluene (a), THF (b), pyridine (c) and H_2SO_4 (d) (C ~ 5.25–8.74×10^{-5} mol dm^{-3}).

Based on a number of studies [3, 8, 13], we suggested the supramolecular structure of the dimeric complex in which the macrocycles are bonded by coordinating interactions between zinc ion of the first phthalocyanine macrocycle and oxygen atom of the OH-group of the second one. The estimated structure of this compound should provide high stability and reveal new properties. According to DFT calculations, the slip angle of the macrocycles in the dimer is 22.8° [22]; therefore, it can be considered as a J-type dimer. It is also important to emphasize that the axial coordination leads to an increase in the angle of

slippage (Fig. 2) and, as a result, may even lead to the cofacial arrangement of the macrocycles, which is characteristic of H-aggregates.

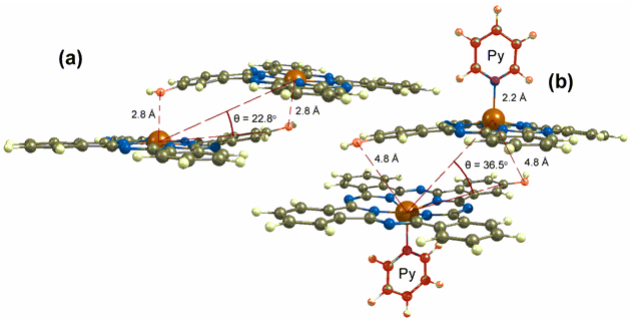

Fig. 2. DFT-optimized structures (ground state) of the model dimer based on compound **3** (a) and its analog bearing a pyridine molecule as an axial ligand (b).

The observed tendency of the controlled displacement of the macrocycles can later be used to fine-tune the properties of dimeric complexes with a similar structure.

Thermal stability determination

To determine thermal stability of synthesized dimer **3**, thermogravimetric analysis (TG) and differential scanning calorimetry (DSC) were used (Fig. 3).

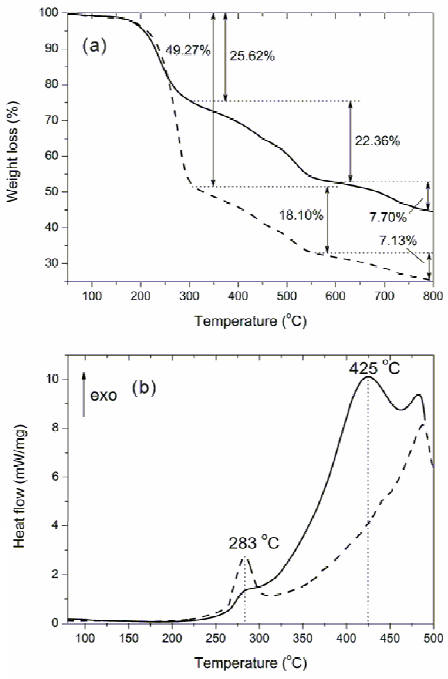

Fig. 3. TG (a) and DSC (b) data for compounds **2** (----) and **3** (——).

As Fig. 3a shows, the destruction behavior of the monomer complex was similar to that of the dimer **3**, which indicates their overall equal stability. However, the first step on the TG curve in the case of monomer **2** indicated double weight loss in comparison to dimer **3**, which also correlated with a greater heat effect on the DSC curves (Fig. 3b). In our previous work [22] it was shown that for OH-containing phtalocyanines, such a result (at 250-300°C) is due to thermal elimination of peripheral substituents. One can assume that, in the case of monomer complex **2**, this process will proceed to a greater degree because of the fact that the intermolecular contacts in the macrocycles are not as strong as those in dimer **3**. The second continuous heat effect (at 300-450°C) can be attributed to the dimer decomposition, with the peak at 425°C corresponding to the maximum rate of the process. However, it is practically impossible to separate the processes of coordination bond breakage with monomer formation and the destruction of the macrocycle, so we cannot calculate the heat effect of dimer to monomer transformation. The main reason is the uncontrolled variation of the system composition and heat capacity during thermal decomposition, which is difficult to estimate. The other reason is due to the strong overlap of the peaks of peripheral substituent elimination and those of breaking of Zn...O bonds and further destruction of the macrocycles.

To evaluate the possibility of dimer destruction, a hypothetical parallel distancing of the macrocycles was simulated. Scanning the potential energy surface (PES) along the distance between zinc atoms with a step size of 0.1 Å allowed us to show a fairly significant energy barrier (> 100 kcal/mol), which is possible to overcome only with full distortion and destruction of the macrocycles. It follows that the thermal decomposition of the dimer is initially performed by the relative shifting of the macrocycles in parallel planes. As a result, the forces of the intramolecular interactions between the macrocycles binding a dimer should weaken. Subsequently, both parts of the dimer begin to exhibit properties similar to the case of monophthalocyanines during thermal decomposition. Namely, this stage is the dissociation of the dimer to form monomers. In the present study, the excellent thermal stability of the *double-coordinated* dimeric phthalocyanine complex has been demonstrated for the first time and is essential for the applicability expansion of this class of macroheterocyclic compounds.

UV–Vis and fluorescence study

In contrast to the examples described in the literature, we did not find high sensitivity of the UV–Vis spectra to the nature of the solvent (Fig. 1). Even in concentrated sulfuric acid, the UV–Vis pattern of complex **3** did not virtually change. Thus, the red-shift of the main absorption bands in **3** was observed upon protonation. This process is reversible. Following deprotonation led to quantitative isolation of **3** having original spectral characteristics. The stability of protonated dimeric molecules of complex **3** can be explained by the presence of specific interactions between the involved macrocycles, which exceed the strength of like-charged subunit repulsion. In pyridine, the Q- bands of complexes **2** and **3** (Fig. 1c) are observed at the same wavelength (682 nm), which can be attributed to solvatochromic effect and extra coordination of a pyridine molecule. This is confirmed by DFT calculations for the ground state at PBE level of the theory, which shows that the HOMO–LUMO gap is almost the same for **2**•Py and **3**•$(Py)_2$ (1.36 and 1.37 eV correspondingly). For the dimer, the J-band is observed at 705 nm in pyridine and indicates that the dimer does not collapse as usually occurs with similar compounds [3, 5, 7, 14]. Addition of 4-dimethylaminopyridine (DMAP) to this solution

followed by refluxing for 1 day does not also lead to dissociation of the dimeric compound, demonstrating the same nature of the UV–Vis spectrum of **3** as is in other solvents (Supporting information, Fig. S8).

Previously, we have assumed a coordinating interaction between complexed zinc ions and oxygen atoms of the OH groups. Such coordination should contribute to additional electronic interaction of the macrocycles. It is well-known that the electronic interactions of a complexed metal with a macrocycle correspond to the appearance of additional absorption bands in the electronic spectra in the range of 200-300 nm [23]. We found characteristic absorption band at 287 nm in THF for complexes **2** and **3**, respectively. Applying of the fluorescence measurements allowed us to find a close relationship of this band with the electronic structure of compounds **2** and **3**.

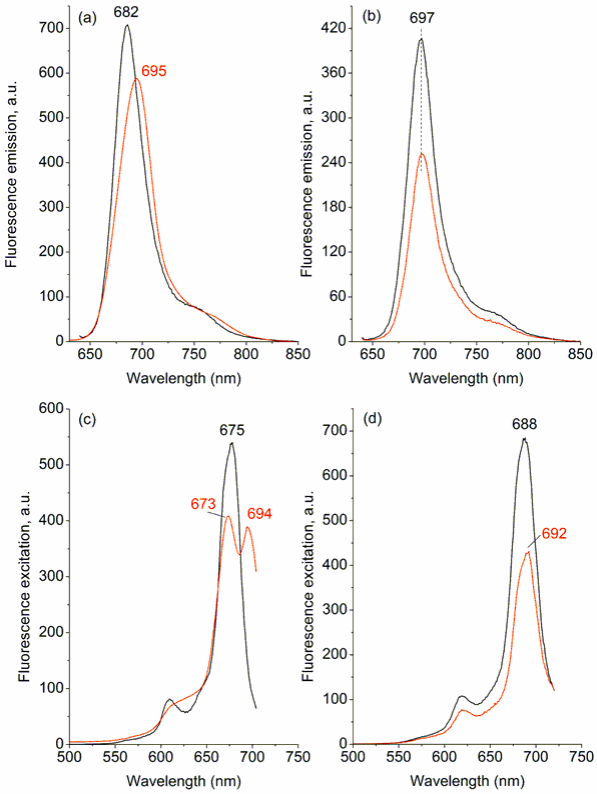

Fig. 4. Fluorescence emission (λ_{ex}=345 nm – *a*, λ_{ex}=630 nm – *b*) and excitation (λ_{em}=715 nm – *c*, λ_{em}=730 nm – *d*) spectra of compounds **2** (black line) and **3** (red line) in THF (a,c) and pyridine (b,d) at C~2.2×10^{-6} mol dm^{-3}.

The shapes of the fluorescence emission spectra while excited in the range of 345–680 nm for test compounds were narrow and clearly resolved (Fig. 4). These spectra are typical of phthalocyanines [21], with Stokes shifts ranging from 7 (for monomer **2**) to 22 nm (for dimer **3**) in THF solution (Fig. 4a,c). At the same time, the emission band of the dimer was red-shifted compared to the monomer by 13 nm, which is in agreement with published data [3]. We can not exclude the fact that the excitation of the dimeric molecule may lead to redistribution of the energy both within and between the macrocycles. As a consequence, certain alterations of the geometry are also possible for dimer **3** due to the change of slip angle. This fact should result in a partial quenching of the fluorescence and decreasing of the fluorescence quantum yield (Φ_F) in comparison with the monomer. Indeed, the Φ_F of dimer **3** in 1.5–3 times smaller compared to monomer **2**, depending on the solvent nature. This result somewhat differs from the available literature data [14], and may be attributed to the flexibility of the structure in the S_1 state similar to other self-assembled phthalocyanines in the ground state [4, 24].

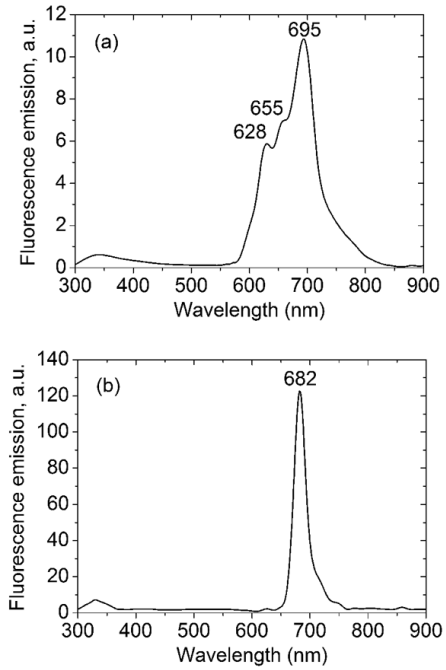

Fig. 5. Fluorescence emission spectra of **3** (a) and **2** (b) in THF while excited at 287 nm.

Special attention should be paid to the complicated nature of the emission spectra of dimer **3** when excited in the UV region (λ_{ex} = 287 nm in THF). The emission band is broadened and splitted (Fig. 5) unlike monomer. RHF–CIS calculations (S_1 state, see Supporting information for details) allowed us found a large structural change between the ground and excited states and the fact that the metal is displaced from the core of the phthalocyanine ring upon excitation. Distortion of the macrocycles in the dimer is found to be increased with the distance from the center of the macrocycles which is due to the fact that the electronic density is shifted to the area of effective contact of the macrocycles. So, the dimer behaves as a complicated molecule with a separated electronic density. The addition absorption bands in the range of 200-300 nm were found to characterize charge transfer processes in phthalocyanine complexes [23]. In our case the absorbance at 287 nm can be associated with n–π* transitions, namely, with the transfer of the free electron pair of oxygen atom of hydroxy group to the macrocyclic system. Consequently, the nature of the emission spectrum of the dimer (Fig. 5) should clearly demonstrate a tendency to exchange electronic density between the two macrocycles. In turn, this is possible with additional electronic connecting contacts between the macrocycles. Unlike dimer **3**, the nature of the monomer **2** emission spectrum in the range of 550-800 nm is essentially independent on the fluorescence

excitation wavelength. Compound **2** also does not reveal any noticeable geometry distortions in the S_1 state.

When studying the fluorescent properties of dimer **3** in pyridine, we found a significant decrease in the Stokes' shift of up to 5 nm, which is almost the same for monomer **2** under similar conditions (Fig. 4b). Moreover, the maximum of the emission band while excited at 630 nm was observed for both compounds at a single wavelength, i.e. 697 nm, with the nature of the excitation spectra for both compounds was similar. Only red-shifting the fluorescence excitation band by 4 nm for dimer **3** was observed (Fig. 4d). This result can be attributed to the fact that the axial coordination of pyridine leads to a weakening of the intramolecular contacts of the macrocycles in the dimer on excitation. According to the RHF–CIS calculations, in the S_1 state the macrocycles are shifted with an increase in the slip angle from 19.7 to 35.8°. Also a slight increase in the Φ_F by 2% for dimer **3** was evidenced, whereas Φ_F of monomer **2** decreased by 13.8%. For this reason, we can not exclude the possibility of the reversible dissociation of the dimeric molecule upon excitation. Since the ground state electronic spectrum of dimer **3** does not depend on the solvent nature, the assumed dissociation can only proceed upon excitation. To estimate this, special investigations will be provided later.

Redox properties investigation

The electrochemical properties of monomer **2** and dimer **3** were investigated in DCB by cyclic voltammetry (CVA). The results are presented in Table 1 and Fig. 6. The anodic shift of the oxidation Ox_1 and reduction Red_1, Red_2 peaks in **3** indicates greater stabilization of the HOMO and LUMO orbitals in the dimer compared with the monomer. Apparently, this is due to the effective intramolecular interaction between the macrocycles in the dimer. Another feature of the behavior of dimer **3** is impaired reversibility of the first oxidation redox transition, which may be due to changes in the spatial arrangement of the macrocycles upon oxidation. In the area of 1.3–1.4V for both compounds, poorly defined peaks of irreversible oxidation Ox_2 accompanied by a small peak at 1.1 (Ox_2') were observed, which may be caused by the oxidation of OH groups. Such irreversibility of the second oxidation step is also characteristic for typical monomeric phthalocyanines [25]. Altogether our data show significant difference in electrochemical properties of the dimer comparing to the monomer and additionally confirm that the dimer is the individual compound (see also Fig. S9, Supporting information).

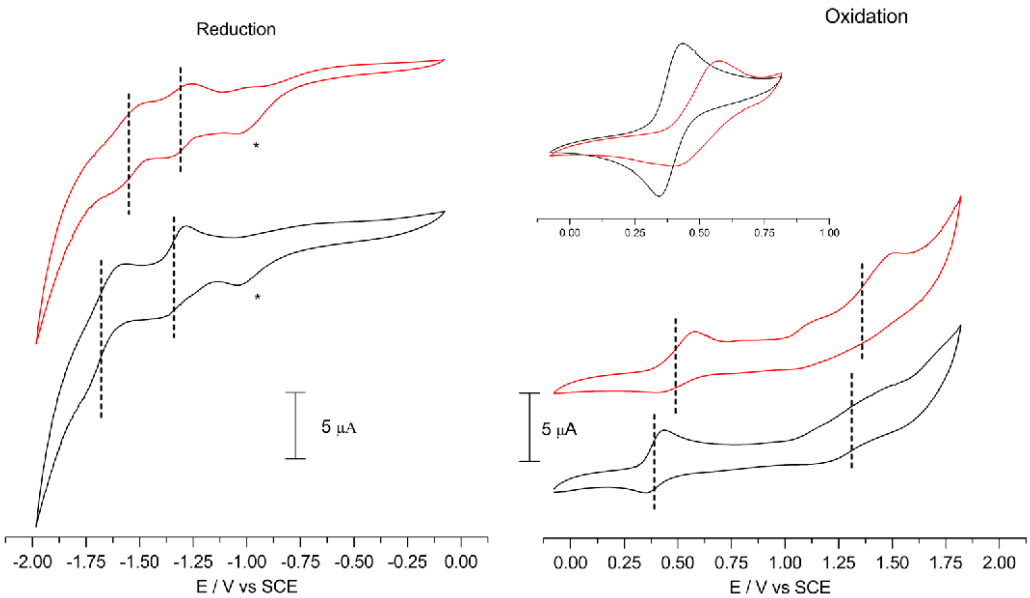

Fig. 6. CVA for monomer complex **2** (black) and dimer **3** (red) in DCB containing 0.15M $[BuN_4][BF_4]$. Peaks indicated by asterisks were due to traces of oxygen. Scan rate 0.1 V/s.

Table 1. Oxidation and reduction potentials E^o/V (vs. Fc/Fc^+) in DCB.

Compound	Red_2	Red_1	Ox_1	Ox_2' [a]	Ox_2 [a]	Ox_1-Red_1
Monomer (**2**)	-1.68(-2.17)	-1.34(-1.83)	0.39(-0.10)	1.12(0.63)	1.31(0.82)	1.73
Dimer (**3**)	-1.55(-2.04)	-1.31(-1.80)	0.49(0.00)	1.11(0.62)	1.36(0.87)	1.80

[a] half-height potentials are given

Conclusions

In this study, a highly stable *double-coordinated* dimeric zinc phthalocyanine complex, firstly synthesized in our research group, has been investigated. By TG/DSC, the limit of thermal

stability was determined (425°C). It was shown that the nature of the solvent and even concentrated sulfuric acid, does not significantly affect the dimeric complex according to the UV–Vis spectroscopy data. All of this clearly evidences on the excellent chemical and thermal stability of this dimeric complex, based on coordinating bonds and π–π electronic interactions. Presence of such interactions was demonstrated by fluorescence emission and excitation spectra in comparison with the UV–Vis spectra. DFT and RHF–CIS calculations were performed for the first time for this kind of molecules, which together with the fluorescence measurements revealed that on excitation, the total electronic system divides into conjugated chromophores, demonstrating the significant interaction between the macrocycles. The existence of specific intramolecular contact was also confirmed by the electrochemical studies.

Acknowledgements

The research was supported by RFBR (Grant No. 12-03-00774), programs of Presidium of RAS as well as by Council under the President of the Russian Federation for State Support of Young Scientists and Leading Scientific Schools (Grant MK-6590.2013.3) and the UFC of MSU under financial support of the Ministry of Education and Science of Russian Federation (Contract N16.552.11.7081). The authors also thank Joint Supercomputer Center of RAS (www.jscc.ru) for providing computing resources.

Notes and references

[a] Institute of Physiologically Active Compounds, Russian Academy of Sciences, 142432 Chernogolovka, Moscow Region (Russian Federation)
[b] Department of Chemistry M. V. Lomonosov Moscow State University, 119991 Moscow (Russian Federation)

† Electronic Supplementary Information (ESI) available: characterization, theoretical calculations and addition experiments. See DOI: 10.1039/b000000x/

‡ Corresponding author. Tel.: +7 496 5242566, e-mail address: tolbin@inbox.ru (Dr. A.Yu. Tolbin).

1. N. Kobayashi, *Coordin. Chem. Rev*, 2002, **227**, 129-152.
2. H.S. Nalwa, ed., *Supramolecular Photosensitive and Electroactive Materials*, Academic Press, San Diego, 2001.
3. V. Novakova, P. Zimcik, K. Kopecky, M. Miletin, J. Kunes, K. Lang, *Eur. J. Org. Chem.*, 2008, **19**, 3260-3263.
4. K. Ishii, S. Abiko, M. Fujitsuka, O. Ito, N. Kobayashi, *J. Chem. Soc., Dalton Trans.*, 2002, 1735–1739.
5. X. Huang, F. Zhao, Z. Li, Y. Tang, F. Zhang, C.-H. Tung, *Langmuir*, 2007, **23**, 5167-5172.
6. M. Morisue, H. Fukui,M. Shimizu,K. Inoshita,Y. Morisaki, Y. Chujo, *Tetrahedron Lett.*, 2014, **55**, 271-274.
7. F. Cong, J. Li, C. Ma, J. Gao, W. Duan, X. Du, *Spectrochimica Acta Part A*, 2008, **71**, 1397-1401.
8. K. Ishii, M. Iwasaki, N. Kobayashi, *Chem. Phys. Lett.*, 2007, **436**, 94-98.
9. X.-Fu Zhang, Q. Xi, J. Zhao, *J. Mater. Chem.*, 2010, **20**, 6726-6733.
10. X. Huang, F. Zhao, Z. Li, L. Huang, Y. Tang, F. Zhang, C.-H. Tung, *Chem. Lett.*, 2007, **36**, 108-109.
11. K. Adachi, H. Watarai, *J. Mater. Chem.*, 2005, **15**, 4701-4710.
12. K. Ishii, Y. Watanabe, S. Abiko, N. Kobayashi, *Chem. Lett.*, 2002, 450-451.
13. L. Niu, C. Zhong, Z. Chen, Z. Zhang, Z. Li, F. Zhang, Y. Tang, *Chin. Sci. Bull.*, 2009, **54**, 1169-1175.
14. K. Kameyama, M. Morisue, A. Satake, Y. Kobuke, *Angew. Chem. Int. Ed.*, 2005, **44**, 4763-4766.
15. A.Yu. Tolbin, V.E. Pushkarev, I.O. Balashova, L.G. Tomilova, *Mendeleev Commun.*, 2013, **23**, 137-139.
16. A.Yu. Tolbin, L.G. Tomilova, and N.S. Zefirov, *Mendeleev Commun.*, 2008, **18**, 286-288.
17. A.T. Gradyushko, A.N. Sevchenko, K.N. Solovyov, M.P. Tsvirko, *Photochemistry and Photobiology*, 1970, **11**, 387-400.
18. M. Erznzerhof, G.E. Scuseria, *J. Chem. Phys.*, 1999, **110**, 5029.
19. D. N. Laikov, Yu. A. Ustynyuk, *Russ. Chem. Bull., Int. Ed.*, 2005, **54**, 820-826.
20. K. Ishii, N. Kobayashi, *The Photophysical Properties of Phthalocyanines and Related Compounds, in The Porphyrin Handbook (eds. K.M. Kadish, R. Guilard, K.M. Smith), Academic Press*, 2003, **16**, 1-42.
21. T. Nyokong, E. Antunes, *Photochemical and Photophysical Properties of Metallophthalocyanines, in the Handbook of Porphyrin Science (eds. K.M. Kadish, K.M. Smith, R. Guilard), World Scientific Press*, 2010, **7**, 247-357.
22. A.Yu. Tolbin, V.E. Pushkarev, V.B. Sheinin, S.A. Shabunin, L.G. Tomilova, *J. Porphyrins Phthalocyanines*, 2014, **18**, 155-161.
23. T. Fukuda, N. Kobayashi, *UV-Visible Absorption Spectroscopic Properties of Phthalocyanines and Related Macrocycles, in the Handbook of Porphyrin Science (eds. K.M. Kadish, K.M. Smith, R. Guilard), World Scientific Press*, 2010, **9**, 1-644.
24. M. Kimura, T.Kuroda, K. Ohta, K. Hanabusa, H. Shirai, N.Kobayashi, *Langmuir*, 2003, **19**, 4825-4830.
25. T.V. Dubinina, S.A.Trashin, N.E. Borisova, I.A. Boginskaya, L.G.Tomilova, N.S.Zefirov, *Dyes. Pigm.*, 2012, **93**, 1471-1480.